Comparative Studies for the Assessment of the Quality of Near-Real-Time GPS-Derived Atmospheric Parameters

R. Pacione

Telespazio S.p.A–Centro di Geodesia Spaziale, Matera, Italy

F. Vespe

Agenzia Spaziale Italiana–Centro di Geodesia Spaziale, Matera, Italy

(Manuscript received 31 October 2006, in final form 30 August 2007)

ABSTRACT

Accurate and frequent sampling of atmospheric parameters, such as water vapor, is important for enabling reliable weather forecasts and global climate studies over a wide range of spatial and temporal scales. Recent developments in global positioning system data processing have allowed the estimation of zenith total delay (ZTD), the delay of the neutral atmosphere, with a high degree of accuracy using continuously operating GPS networks. From this delay integrated water vapor can be derived by means of additional meteorological information, in particular observed pressure or numerical weather prediction model pressure. Comparisons with other independent techniques must be performed to evaluate the quality of atmospheric parameters directly estimated or retrieved from the GPS system. In this work the accuracy of GPS atmospheric parameter, namely, zenith total delay, delivered in near–real time from a European ground-based network of permanent GPS receivers has been assessed. It is compared to other GPS solutions, radiosonde profiles, and High-Resolution Limited-Area Model (HIRLAM)-derived ZTD. Intercomparisons between results from different GPS analysis centers in the framework of the Targeting Optimal Use of GPS Humidity Measurements in Meteorology (TOUGH) project show a mean ZTD station bias at the level of ±6 mm with a related standard deviation of about 7–8 mm. In the comparison with radiosondes, an overall ZTD bias of about 7 mm with a standard deviation of 9 mm is detected. Finally, the comparison of ZTD near–real time against the HIRLAM models has an average bias of about −4.8 mm and a standard deviation of 11.5 mm.

1. Introduction

Water vapor is a key element in the hydrological cycle and it is an important greenhouse gas in the atmosphere. The very inhomogeneous and highly variable distribution of atmospheric water vapor makes it a crucial element in weather forecasting. Conventional observing systems such as radiosondes and microwave radiometers have insufficient spatial sampling for observing its high variability. Ground-based GPS provides continuous, high temporal resolution measurements of the zenith total delay (ZTD), from which integrated water vapor can be derived. GPS networks cover all the continents but not the oceans (Bevis et al. 1992). Water vapor can also be estimated from spaceborne GPS receivers orbiting on low earth-orbiting satellites. They can provide high vertical resolution with good global coverage, but the observations are not continuous in time at any geographical location (Kursinski and Hajj 2001). The ground- and space-based GPS techniques complement each other, and their value as an all-weather and self-calibrated remote sensing system of the earth's atmosphere has been proven over the last decade and a half.

Techniques have been developed to acquire, process, and distribute GPS-derived atmospheric parameters, which are useful for numerical weather prediction (NWP) forecasts and climate applications. The atmospheric observable from ground-based GPS data is the ZTD, that is, the additional propagation delay caused by dry air and water vapor in the atmosphere when the GPS signal propagates from the satellite to the receiver.

Corresponding author address: Dr. Rosa Pacione, Telespazio S.p.A–Centro di Geodesia Spaziale, 75100 Matera, Italy.
E-mail: rosa.pacione@telespazio.com

DOI: 10.1175/2007JTECHA935.1

It can be split into a hydrostatic part (ZHD), which is a function of the surface pressure (Saastamoinen 1972), and a wet component, which depends on the water vapor content. ZHD can be easily computed using surface pressure measurements or pressure fields derived from NWP models, and then can be subtracted from the estimated ZTD to provide the zenith wet delay (ZWD). This last is approximately proportional to the integrated water vapor (IWV). The nondimensional factor (Askne and Nordius 1987; Elgered et al. 1991) is a weak function of the weighted mean temperature of the atmospheric column and can be related to the surface temperature by an empirical linear relationship (Bevis et al. 1994; Emardson and Derks 1999).

For NWP applications the goal is to produce ZTD estimates with a reasonable quality and in near–real time (NRT), that is, within 1 h, 45 min from data acquisition.

Since 1999 in the framework of the Meteorological Applications of GPS Integrated Column Water Vapor Measurements in the Western Mediterranean (MAGIC) Project (Haase et al. 2001) at the Space Geodesy Center (CGS) of the Italian Space Agency (ASI), an operational automatic system has been running continuously to deliver GPS tropospheric parameters on a daily basis with 2-week latency (Pacione et al. 2001). In June 2001, ASI joined the European Cooperation in the Field of Scientific and Technical Research (COST)-716 Near Real-Time demonstration phase (Elgered et al. 2005), processing on an hourly basis a European network of about 15 stations (Pacione and Vespe 2003). In February 2003 under the umbrella of the Targeting Optimal Use of GPS Humidity Measurements in Meteorology (TOUGH) project it grew in size, reaching the current network size of 57 stations in June 2006. GPS data are processed at several institutions involved both in COST-716 and in TOUGH to ensure consistent results independent of the software used and the applied strategy. Each analysis center is responsible for retrieving the GPS data, processing them and transferring the ZTD estimates to the project ftp site in NRT to make them available to the meteorological users. In processing the data, the centers include stations from a common reference network to provide a means for cross-checking the quality of the ZTD estimates. Radiosonde observations are used as an important independent dataset for validating GPS ZTD data. The quality of the radiosondes is high, but the temporal and spatial resolutions sometimes lead to problems. High-Resolution Limited-Area Model (HIRLAM) NWP analyses and forecasts are used as another source of independent data for monitoring GPS ZTD. These data are continuously monitored, both to help to improve the product quality and to determine its error characteristics, which must be known when assimilating the data into NWP systems.

In this study we assess the accuracy of GPS-derived atmospheric parameter delivered in near–real time from a European ground-based network. In section 2 we describe the NRT ZTD processing system, which has run continuously for 4 yr, together with an assessment of the ZTD internal consistency. A statistical method to assess the degree of reliability of the NRT ZTD and their real uncertainties is proposed and discussed. In section 3 we compare ZTD at 13 sites with the nearest radiosonde observations that are in operational use in weather forecasting. The results of the validation against the HIRLAM numerical weather prediction model output are described in section 4. Conclusions are drawn in section 5.

2. Near-real-time ZTD data processing system

GPS data from 57 European stations are processed on an hourly basis to provide ZTD to meteorological agencies. The ground-based GPS network (Fig. 1) covers the central Mediterranean area with Italy as the core region.

The GPS-Inferred Positioning System and Orbit Analysis Simulation Software version II (GIPSY-OASIS II; Webb and Zumberge 1997) is used for data reduction with the standard technique of network adjustment. For the NRT solutions, the International GPS Service (IGS; Beutler et al. 1999) ultra-rapid orbits are kept fixed but checked, and "bad" satellites or stations are automatically excluded on the basis of the analysis of postfit-phase observation residuals, as suggested by Springer and Hugentobler (2001). Thus, a noisy station is not analyzed for the next 24 h. A 24-h sliding window approach for data handling is applied with a sampling rate of 5 min and an elevation cutoff angle for the data of 10°. The ZWD is estimated every 5 min with a stochastic model (random walk) and a constraint of 20 mm/($\sqrt{h}$). The station coordinates are kept fixed to values provided by combining 1 month of daily postprocessed (PP) solutions, whose repeatability is at the centimeter level or better (Fig. 2) and are updated every 30 days, taking into account the tectonic movements of the area. A detailed description of the processing strategy is reported in Pacione (2005).

In addition, a postprocessed solution is run on a daily basis with the precise point positioning approach (Zumberge et al. 1997). The main goal of the PP solutions, whose features are reported in Pacione et al. (2001), is to provide both ZTD estimates useful for climate applications and site coordinates to fix in the NRT data

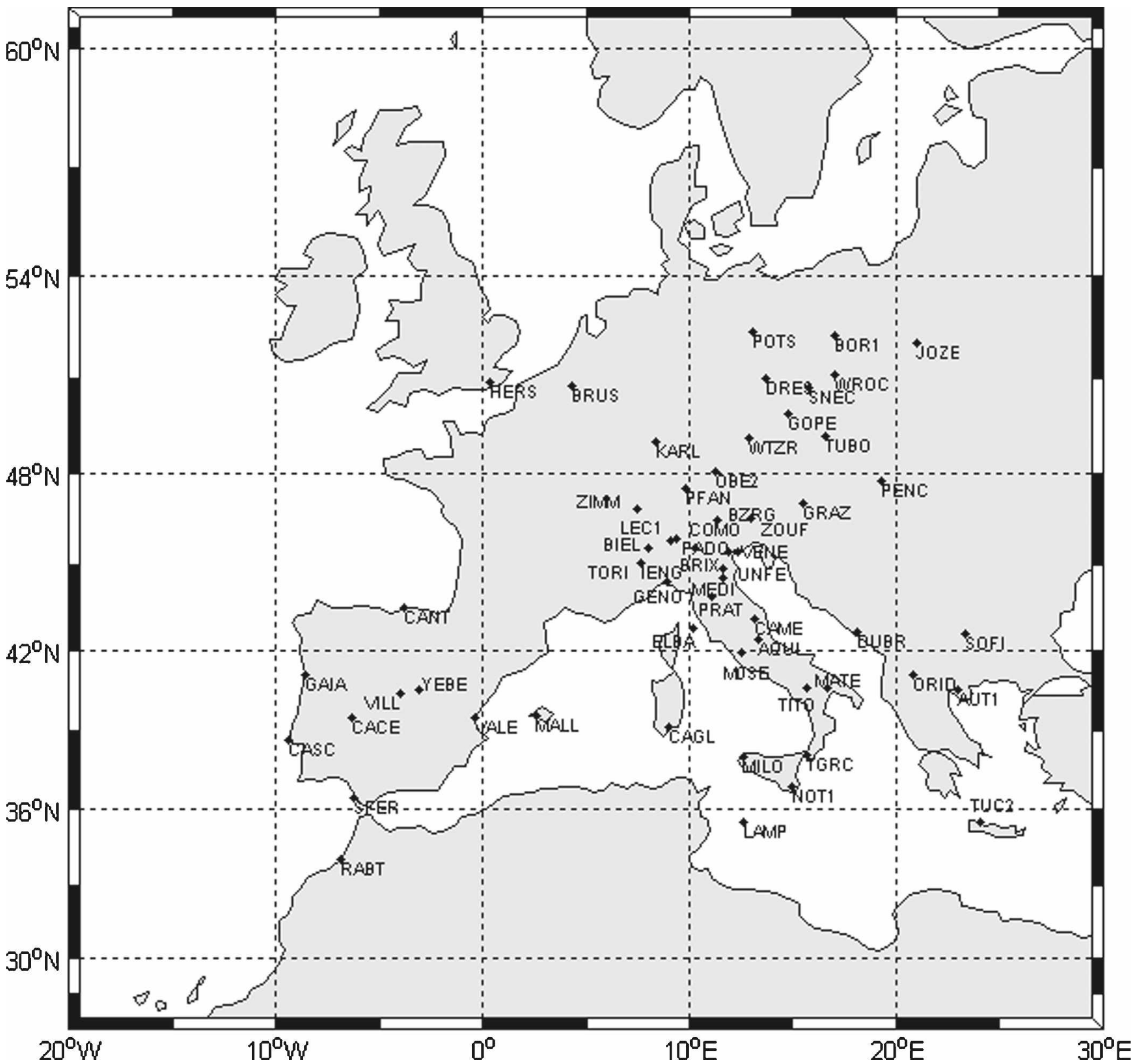

Fig. 1. Ground-based GPS network; June 2006.

processing. An accuracy check of the site coordinates is regularly performed, considering their repeatability as an indicator of the ZTD quality. As a rule of thumb, 9 mm in the height component [i.e., 3 mm in ZTD as explained in Santerre (1991)] are needed to fulfill the requirement of retrieving IWV at an accuracy level of 0.5 kg m^{-2} (Bevis et al. 1994).

The ZTD internal consistency can be seen by comparing NRT and PP ZTD estimates. Figure 3 shows an example of the daily variation in ZTD bias and standard deviation of the residual time series of PP minus NRT for 6 European Reference Frame (EUREF) stations from January 2004 to June 2006. On a daily basis, the PP minus NRT ZTD station bias ranges from -4.9 to -1.9 mm, and the related standard deviation is about 5 mm. Similar results have been obtained in the framework of the COST-716 Action comparing individual NRT solutions to combined postprocessed solutions (Elgered et al. 2005).

a. Comparison between individual NRT solutions

A 2-yr-long time series of 39 EUREF stations (January 2004–December 2005) is used to compare NRT ZTD estimates coming from the following analysis centers involved in the European COST-716 Action and in the TOUGH project: Mécanique Appliquée et Sciences de l'Environnement (ACRI-ST, France); Agenzia Spaziale Italiana (ASI, Italy); Bundesamt für Kartographie und Geodäsie (BKG, Germany); GeoForschungsZentrum Potsdam (GFZ, Germany); Geodetic Observatory, Pecny (GOP, Czech Republic); Institut d'Estudis Espacials de Catalunya (IEEC, Spain); Federal Office

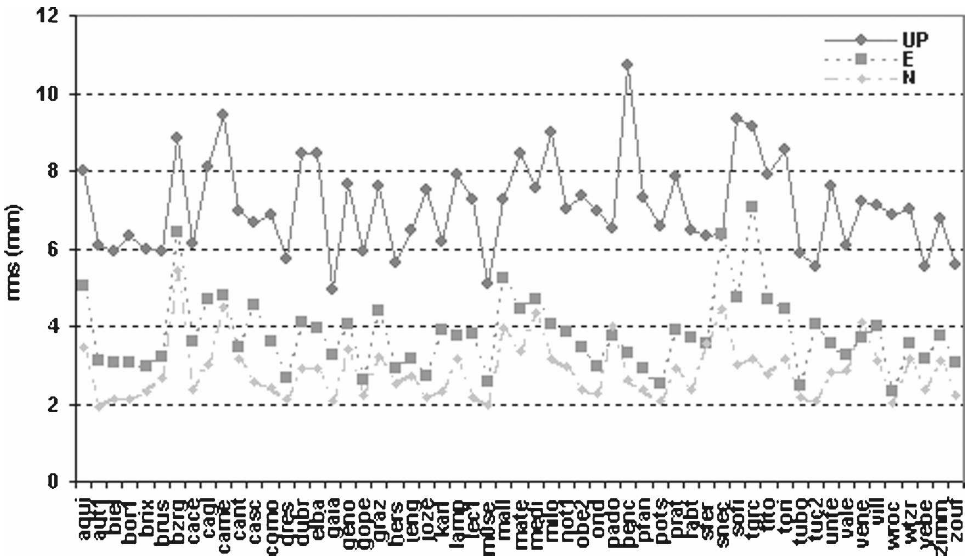

FIG. 2. RMS of the day-to-day scatter in postprocessed site coordinate time series from June 2001 to June 2006 with a linear trend removed. The linear trend is due to tectonic motion, which is accounted for by updating coordinates each month. The stations are in alphabetical order.

of Topography (LPT, Switzerland); Nordic Geodetic Commission Norwegian Mapping Authority (NKG, Norway); Nordic Geodetic Commission (NKGS, Sweden); and Institut Géographique National (SGN, France). We refer to the Elgered et al. (2005) final report for a description of all the processing techniques.

Pairwise comparison of individual NRT solutions show a good agreement over the whole period considering the ASI solution as the reference. The ZTD station bias is between ±6 mm, that is, about ±1 kg m^{-2} IWV. In the comparison gross errors (i.e., values >30 mm) are rejected. The percentage of the rejected data ranges from 9% in the case of GFZ to 1% in the case of BKG. The standard deviation is about 10 mm in the comparisons with respect to SGN, lower (7–8 mm) in all the other comparisons. The obtained results can be considered an indication of the precision which can be now achieved by the GPS techniques.

b. Assessment of the uncertainties of NRT estimates

Comparing ZTD solutions from different analysis centers we realize that the ZTD estimates are very highly correlated; however, there is a poor correlation between the corresponding errors. This means that the ZTD quality indicator obtained by the GPS processing may not be reliable. The formal standard deviation as computed from the inversion of the normal matrices is not a uniform quality indicator since different processing centers use different strategies to compute the ZTD standard deviation and have different detection levels to flag or reject bad data. We apply the method extensively applied to galaxy redshift catalogues (Sandage 1978; Tonry and Davis 1979; Rood 1982) to assess the degree of reliability and the real uncertainties of NRT ZTD. The approach is described in detail below.

If we have two different datasets, x_i and y_i, which are measurements of the same variable in time and space, we can assess the real uncertainties of the measurements that are intrinsically less precise. Let us assume that y_i is more precise than x_i. Then we can define the nondimensional dataset z_i as

$$z_i = \frac{(x_i - y_i)}{\sqrt{\sigma_{x_i}^2 + \sigma_{y_i}^2}}. \qquad (1)$$

If x_i and y_i are unbiased and their internal error is not underestimated, z_i should behave according to a Gaussian distribution with mean $\mu = 0$ and variance $\sigma_z^2 = 1$. The error σ_μ on the mean should behave according to a normal distribution,

$$\sigma_\mu = \frac{\sigma_z}{\sqrt{n-1}}, \qquad (2)$$

where n is the number of measurements. If μ is significantly different from 0 (i.e., more than 3σ), it means that the x dataset is biased. On the other hand, the variance behaves according to the χ^2 function with $n - 1$ degrees of freedom. We must check if the value $\sigma_z^2 = D_z = 1$ is within the variance interval that is determined by fixing the confidence level to 90%.

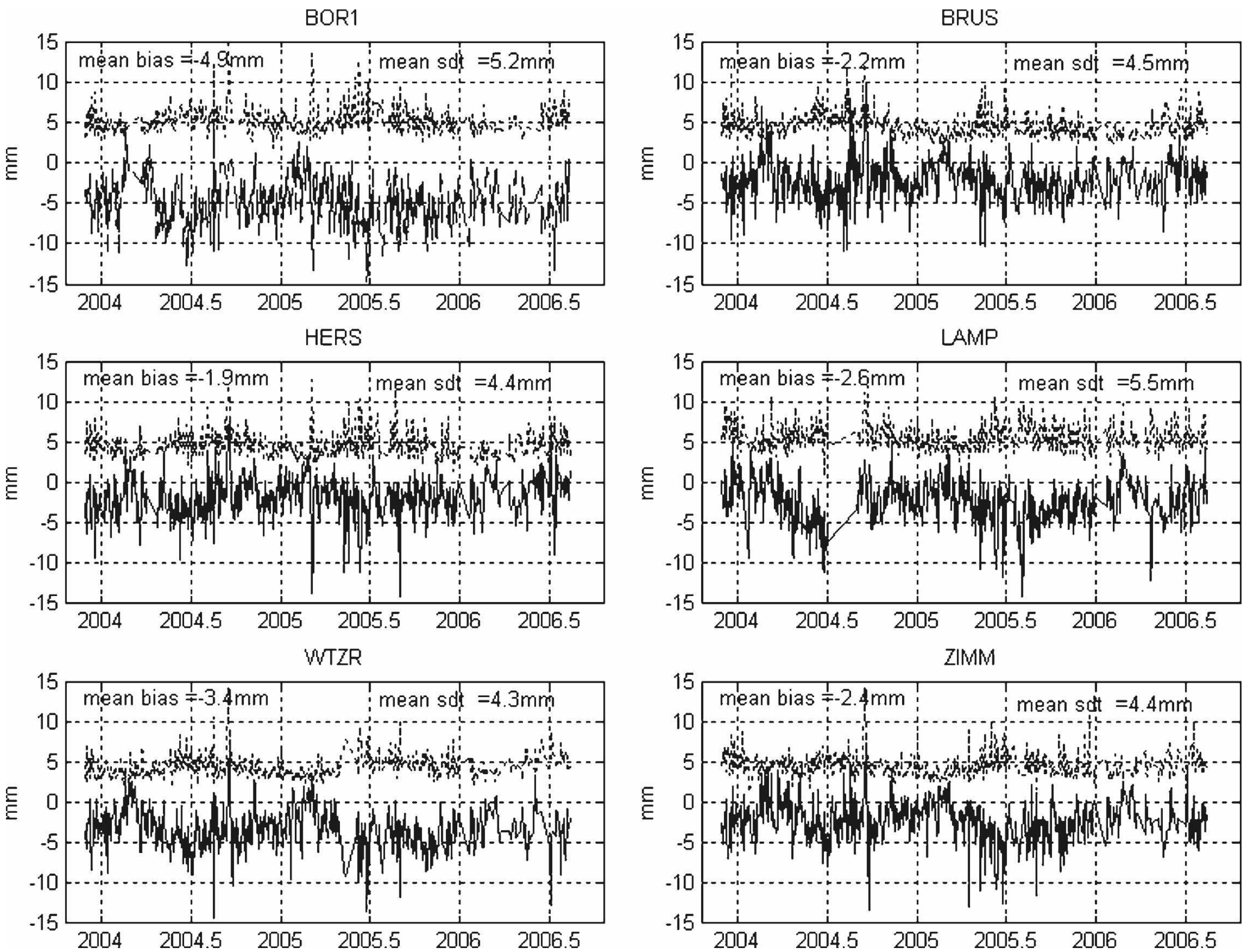

FIG. 3. Daily bias (solid line) and standard deviation (dotted line) of PP minus NRT solutions for the period January 2004–June 2006.

Thus we build another parameter as follows:

$$V = \frac{\tilde{D}(n-1)}{D_{\rm exp}}, \tag{3}$$

where $D_{\mathbf{exp}}$ is the variance for which we want to know the confidence interval, and $\tilde{D}$ is the estimated variance of the z dataset. The parameter V in Eq. (3) behaves according the χ^2 distribution with $n - 1$ degrees of freedom. It is well known that the χ^2 distribution is asymmetric. Thus, the confidence interval at the level of probability β [hereafter CI(β), with β in the present case equal to 0.9] is asymmetric around $\tilde{D}$ as well. In our case, the confidence interval CI(β) of the parameter V is

$$X_1 \le V \le X_2, \tag{4}$$

where $\chi^2(X_1) = [(1 - \beta)/2)]$ and $\chi^2(X_2) = [(1 + \beta)/2)]$.

Thus, merging Eqs. (3) and (4) we get the CI(β) for the variance D:

$$\frac{\tilde{D}(n-1)}{X_2} \le D \le \frac{\tilde{D}(n-1)}{X_1}. \tag{5}$$

Thus, if the nominal value of $D_z = 1$ is outside the range set with Eq. (5), then the variance is biased, either underestimated or overestimated.

We apply this method considering the less accurate x dataset the 96 NRT ZTD time series coming from the different TOUGH analysis centers, and considering the y dataset the EUREF combined tropospheric solution (additional information is available online at http://www.epncb.oma.be/_organisation/projects/trop_sp/index.php). Figure 4 shows the histograms of the z datasets defined in Eq. (1) compared to the Gaussian distribution (black lines) having the same μ and σ of the given series for the Wettzell station (WTZR, Germany) and ACRI, ASI, BKG, GFZ, GOP, IEEC,

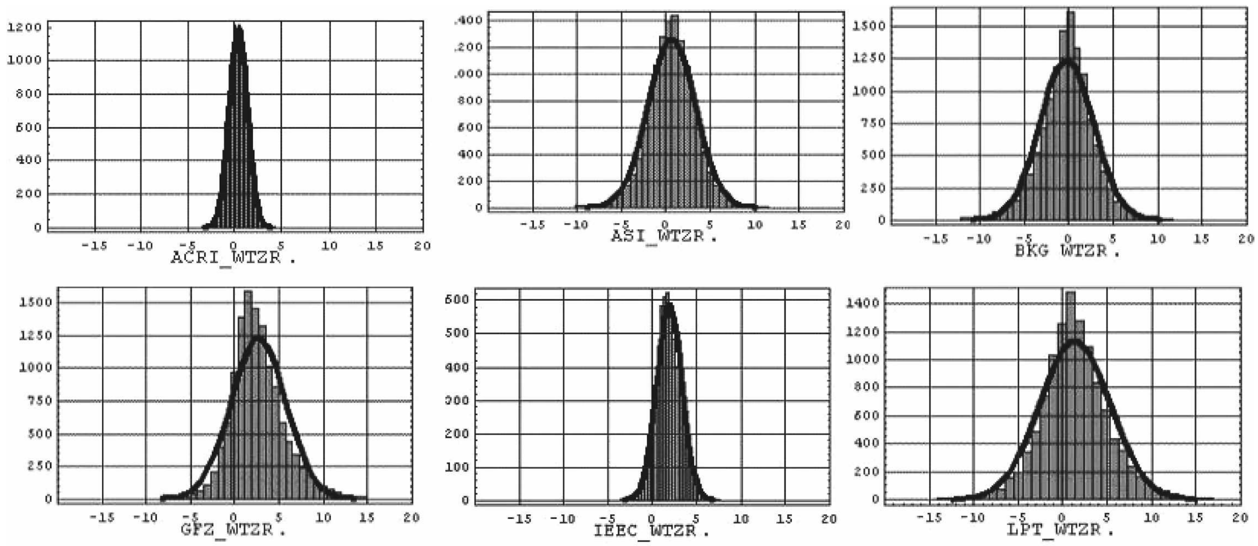

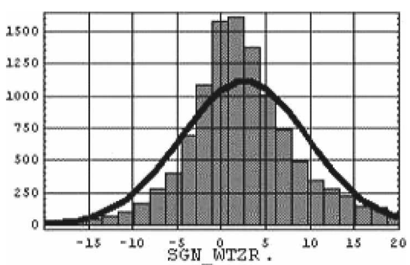

FIG. 4. The y datasets adopted are WTZR EUREF combined ZTD solutions, while the x datasets are ACRI, ASI, BKG, GFZ, IEEC, LPT, and SGN NRT solutions. The black line represents the Gaussian function having the same mean and variance of the x dataset. The nondimensional values of the combined z dataset [see Eq. (1)] and the number of the estimates are reported along the x and y axis, respectively.

SGN, and TOUGH analysis centers. For each distribution we apply the 3σ criterion to the mean of the z variable (Rood 1982). In this test we do not reject any data beforehand as was done in the analysis of residuals in section 2a; however, we do retain the quality control that filters outliers in the data processing chain, in particular by removing stations for a 24-h time period if their phase residuals are large (see section 2). The χ^2 test is applied to determine if the histograms follow a Gaussian distribution fails for most of the dataset. A mean scale factor and scaled sigma are computed for each analysis center and reported in Table 1. We note that all Bernese (Beutler et al. 2007) and GIPSY solutions (BKG, GOP, LPT, SGN, ASI, and IEEC) have underestimated uncertainties and their statistical distribution is not exactly Gaussian; while ACRI solutions using the GPS analysis at the Massachusetts Institute of Technology (MIT) software (GAMIT; Herring et al. 2006) have overestimated uncertainties and their statistical distribution is nearly Gaussian. The uncertainties seem to be correlated more to the analysis strategies (troposphere modeling and estimation process) than to the quality of the stations.

A measure of the quality of the station i is given by the nondimensional quantity

$$\nu_i = \sum_{j=1}^{k} \frac{\sigma_{ij}}{\sigma_j}, \tag{6}$$

where σ_{ij} is the mean value of the σ estimated by the analysis center AC_j for the station i, and σ_j is the mean of the σ estimated for each station by the AC_j.

The station i is considered "good" or "bad" if ν_i, as defined in Eq. (6), is significantly lower or greater than 1. The ν_i value is shown in Fig. 5, where we observe that some stations perform better than others. A detailed investigation into the reasons for individual stations performing poorly is beyond the scope of the paper, but results have been sent to the network operators for

TABLE 1. Mean scaled factor and scale sigma.

	Scaled factor	Scale sigma (mm)
ACRI	0.9	8.3
ASI	2.4	5.6
BKG	2.7	3.2
GFZ	2.8	2.9
GOP	2.8	3.0
IEEC	1.4	7.7
LPT	3.5	3.9
SGN	5.8	3.6

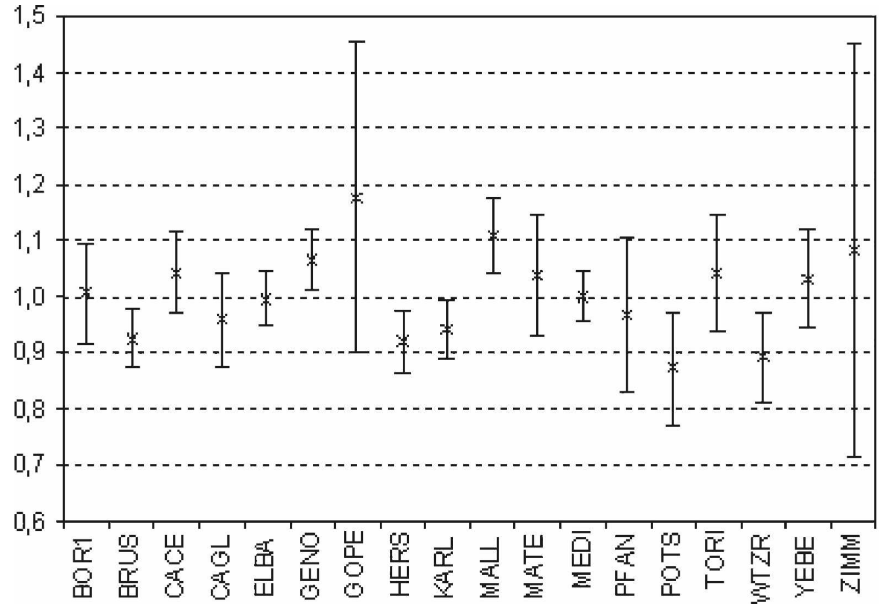

FIG. 5. For each station, the ν_i, as defined in Eq. (6), is reported. The error bar is the standard deviation.

further investigation. The performance of the stations could depend on the quality of the equipment installed (receiver, antenna, internal/external clock) or on the site environment. The approach has been very helpful in singling out stations that have problems that require attention.

3. Comparison of GPS and radiosonde ZTD

GPS- and radiosonde-derived ZTD estimated at 13 sites where nearby radiosonde profiles were available are compared for the period April 2003–June 2006. The selected sites have a latitude ranging from 38° to 50° and a longitude ranging from −4° to 17°, covering most of Europe. Radiosonde profiles come from World Meteorological Organization (WMO) Global Telecommunication Service (GTS), and are provided by the Danish Meteorological Institute in the framework of the TOUGH project as an independent dataset to validate GPS ZTD data. ZTD time series derived from GPS and radiosonde data for two stations, Herstmonceux (United Kingdom) and Milo (Sicily), at different latitudes and with different climatic conditions are shown in Fig. 6. The time series are very consistent and the ZTD annual cycle can be clearly seen. The radiosonde profiles are passed through a program developed in the framework of the MAGIC Project (Haase et al. 2003) that checks the quality of the profiles; converts the dewpoint temperatures to specific humidity; transforms the radiosonde profile to correct for the altitude offset between the GPS and the radiosonde sites; and determines ZTD, ZWD, and IWV, compensating for the change of gravitational acceleration g with height. We select GPS and radiosonde site with separation less than 60 km. The atmospheric state might be slightly different between the two sites and might limit the level of agreement between the two types of measurements; however, there is no direct correlation between the bias and either the horizontal distance or the difference in altitude (see the column distance in Table 2) between the GPS and the radiosonde launch sites.

In Fig. 7 the mean and standard deviation of the residuals between GPS- and radiosonde-derived ZTD are shown. The mean and standard deviation are computed for each station and each month. Looking at the bias we note that the radiosondes are drier than GPS. All of the radiosondes used are Vaisala except at Zimmerwald where Meteolabor radiosondes are launched. The Vaisala dry bias is well known in the literature and has been discussed by Wang et al. (2002), Turner et al. (2003), and Vömel et al. (2006).

The standard deviation has a seasonal dependence, which seems to fit the atmospheric thermal cycle. It is about 10 mm in summer and 7 mm in winter. Such a seasonal variation is confirmed by comparing the standard deviation against the mean, the relative change is 140% in summer and 80% in winter. The overall bias and standard deviation are 7 and 9 mm, respectively. For some sites the standard deviation is near the level obtained in the comparisons carried out between dif-

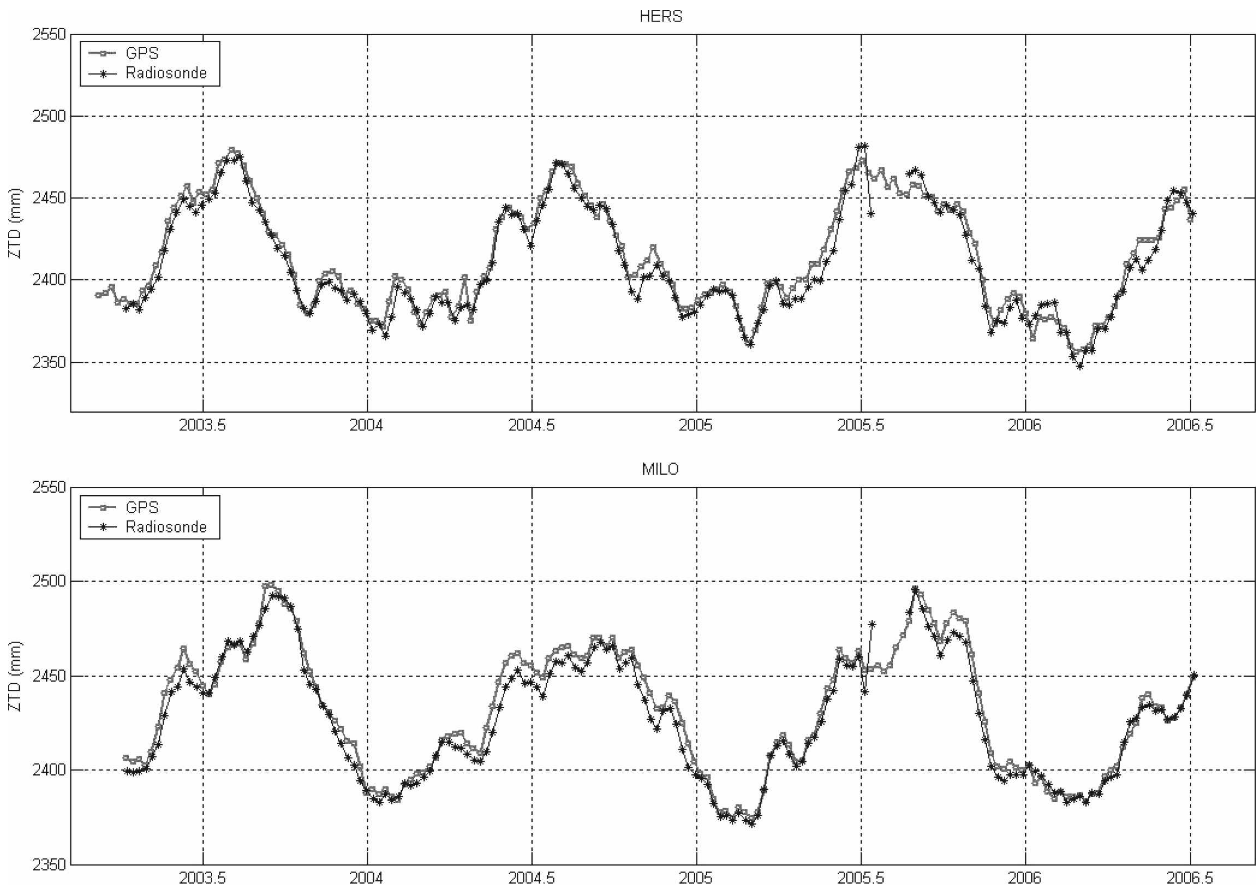

FIG. 6. Herstmonceux (United Kingdom) and Milo (Sicily) from April 2003 to June 2006: GPS (gray line and circle) and radiosonde (black line and asterisk) running mean over 28 days.

ferent analysis centers (ACs), that is, 7–8 mm, indicating that the agreement is within the limit of the precision of the GPS technique. Over 2 years of data, the difference between radiosonde and GPS ZTD estimates delivered in postprocessing mode has a standard deviation of 12 mm of delay and a bias of 7 mm of delay (Haase et al. 2003). In the present study we have an improvement in the standard deviation of the delay,

TABLE 2. Near-real-time GPS ZTD minus radiosonde (RS) comparison table for the period April 2003–June 2006. Distance is the horizontal distance between the radiosonde launch and the GPS antenna, (GPS-RS) height is the altitude difference between the radiosonde launch and the GPS antenna.

GPS site	RS code	Distance (km)	(GPS-RS) height (m)	No. of data	Bias (mm)	Std (mm)	Correlation coefficient
Cagliari, Italy (CAGL)	16560	15	187	1893	6.3	10.3	0.97
Santander, Spain (CANT)	08023	59	−9.7	861	10.3	11.1	0.79
Pecny-Ondrejov, Czech Republic (GOPE)	11520	29	181.4	3090	5.9	7.1	0.94
Herstmonceux, United Kingdom (HERS)	03882	4	−21	1582	4.4	7.8	0.91
Medicina, Italy (MEDI)	15144	15	−1	1167	9.43	8.7	0.97
Trapani-Milo, Italy (MILO)	16429	12	35	2644	2.5	10.1	0.8
Rome, Italy (MOSE)	16245	27	40	846	2.3	9.8	0.97
Oberpfaffenhofen, Germany (OBE2)	10868	27	107	833	11	7.8	0.96
Torino, Italy (TORI)	16113	59	−123	985	9.4	9.3	0.96
Villafranca, Spain (VLL)	08221	32	−38	674	6.6	8.6	0.85
Yebes, Spain (YEBE)	08221	45	288	1159	9.1	8.9	0.84
Wroclaw, Poland (WROC)	12425	13	18	965	10.9	6.8	0.96
Zimmerwald, Switzerland (ZIMM)	06610	40	417	1484	9.8	9.2	0.96

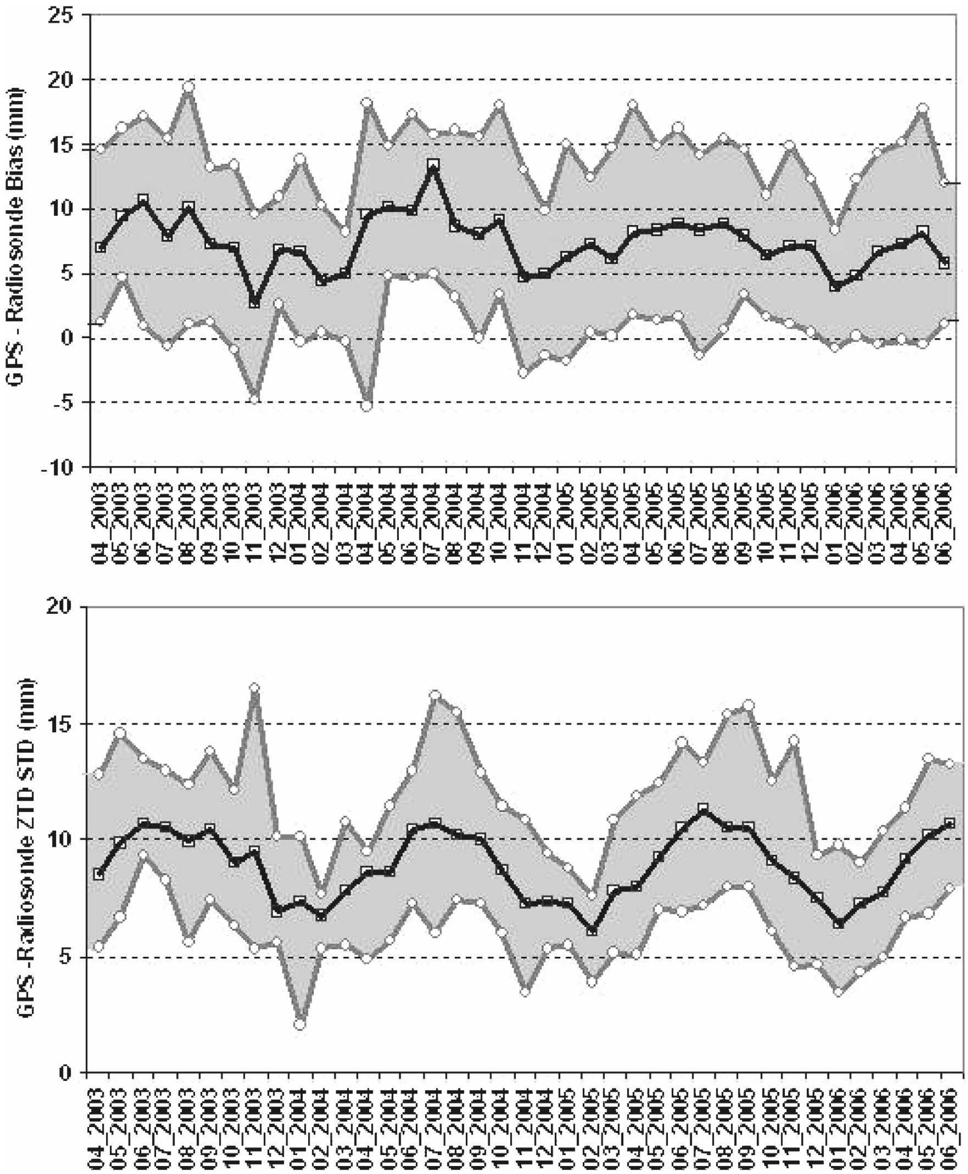

FIG. 7. Monthly variation in (top) ZTD bias and (bottom) std dev of GPS vs radiosonde for all the stations (black line). The gray area lies between the minimum and maximum values.

although in the comparisons we used GPS near-real-time ZTD estimates. The precision of the GPS ZTD estimates (approximately 7 mm) is comparable based on previous comparisons among analysis centers (Haase et al. 2003). It is possible that the improvement in agreement in the last 2 yr is due to improved algorithms for the radiosonde reporting that now consider the dry bias. On the other hand, it may be an indication of the recent improvement in the GPS technique used for remote sensing of the earth's atmosphere and some inconsistency in the measurement of technique precision in the past.

A night/day bimodal distribution of the residuals is detected. We compute midday and midnight bias and standard deviation (Fig. 8) comparing noon and midnight GPS ZTD with respect to radiosonde profiles for each station. The values in Fig. 8 are quite different from those in Table 2, and this is due to the different averaged period taken into account for the computation.

There is no meaningful difference in the standard deviation; while the midday bias of the GPS–radiosonde differences is higher than the midnight one. This bimodal distribution of the day-to-night bias has

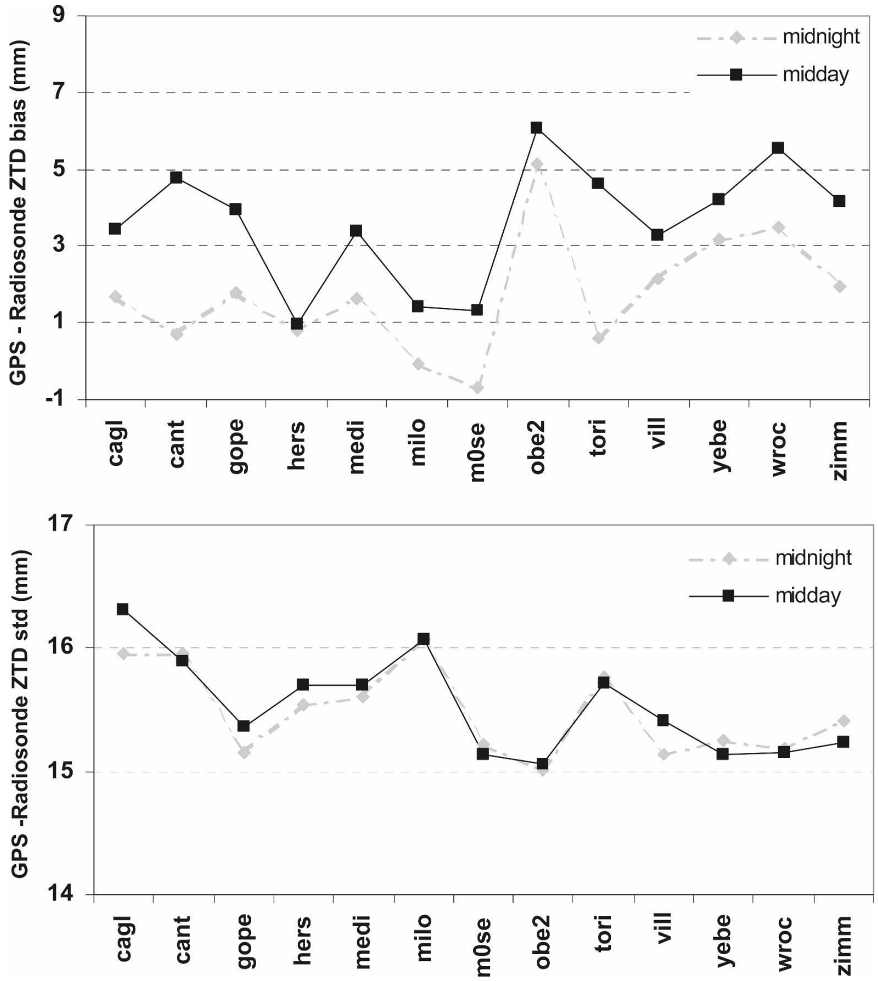

FIG. 8. Midday (square and continuous black line) and midnight (diamond and gray dash–dot line) (top) bias and (bottom) std dev from the GPS ZTD vs radiosonde comparison.

been discussed in Haase et al. (2003) where they propose that it is due to the day–night humidity bias present in the radiosonde measurement (WMO 1996) because of radiational heating of the sensor, rather than a humidity bias related to GPS measurements. Similar bimodal distributions of the GPS and radiosonde residuals have also been observed by Ohtani and Naito (2000) using observations in Japan, Guerova et al. (2005) using observations in Switzerland, and Van Baelen et al. (2005) using observations in France.

4. Comparisons of GPS-derived ZTD with the HIRLAM NWP

We compare GPS-derived ZTD with the Danish Meteorological Institute (DMI) version of the HIRLAM model from May 2003 to June 2006. HIRLAM data come from the numerical weather prediction model used operationally at DMI and can be influenced by the quality of the model itself. The resolution of the model is 0.15° in both horizontal directions, and it has 40 vertical levels. It covers roughly a quarter of the globe including Europe and areas beyond to the west and north. In the framework of the TOUGH project, the model is run with data assimilation every 3 h and the output is available with a resolution of 1 h. GPS and HIRLAM ZTD time series for 2004 are shown in Fig. 9 for the Brussels, Belgium, site (BRUS). The results of the comparison between GPS and HIRLAM ZTD are shown in Fig. 10 where bias and standard deviation are computed for each station with data from May 2003 to June 2006. The bias for most sites is about −4.7 mm, outlining that GPS-derived ZTD is lower than HIRLAM. Haase et al. 2003 found a positive bias of 3.4 mm whereas we find a negative bias of −4.7; however,

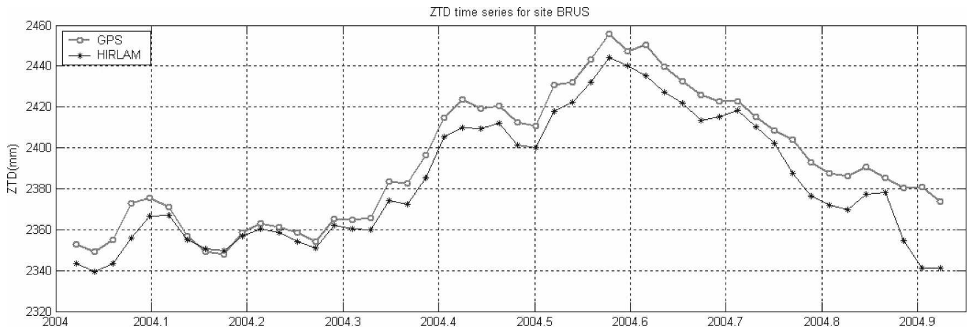

FIG. 9. ZTD 1-yr time series for site BRUS: GPS (gray line and circle) and HIRLAM (black line and asterisk) running mean over 28 days.

these are both smaller than the precision of the GPS ZTD technique and may not be significant.

The standard deviation for most sites is about 11.6 mm with an improvement of about 3% with respect to previous comparisons (Haase et al. 2003). This is to be expected, now that the GPS ZTD data is actually assimilated in the model.

Once again mean and standard deviation of the residuals between GPS and HIRLAM ZTD (Fig. 11) are computed for each station and each month. A seasonal signal emerges from the residual time series with a standard deviation higher in summer than in winter. The monthly ZTD standard deviation increases from about 5 mm in winter to about 15 mm in summer.

Furthermore, we have analyzed the statistical distribution of the residuals between HIRLAM and individual NRT estimates (see section 2b). We do not observe any analysis center or station having systematically lower or higher residuals, indicating that these types of differences are smaller than the remaining error in the HIRLAM analysis.

5. Summary

The ground-based GPS technique is a useful tool for monitoring atmospheric parameters and for capturing their temporal variability. Data from European permanent sites are processed in near-real-time mode, and the estimated ZTD is validated against other GPS estimates delivered in the framework of the TOUGH project. The dataset covers different climatic conditions varying from Alpine to Mediterranean. Comparisons between individual NRT solutions from different analysis centers show good agreement with a delay bias of ±6 mm and a standard deviation of 7–8 mm. A new approach is proposed in order to assess the real uncer-

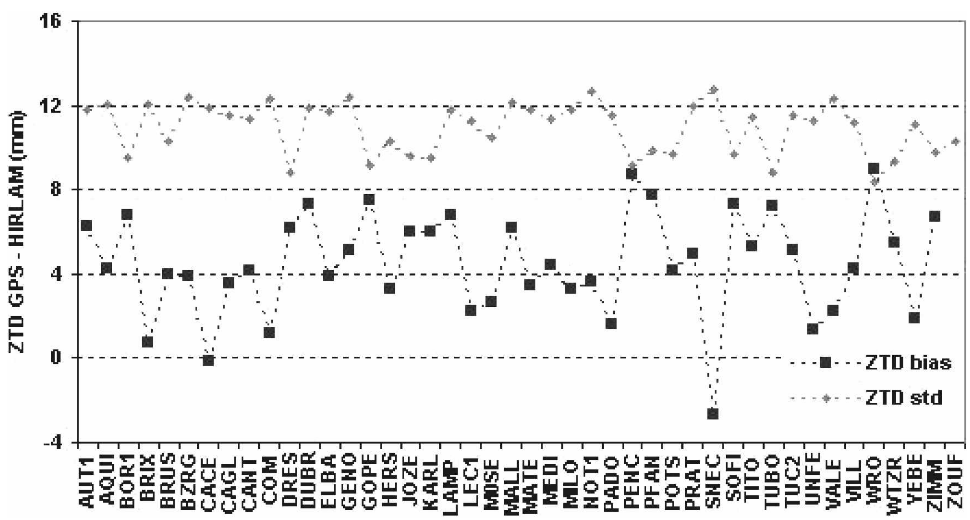

FIG. 10. Bias and std dev of the difference between NRT GPS-derived ZTD and HIRLAM ZTD for each station. All solutions delivered from May 2003 to June 2006. The stations are in alphabetical order.

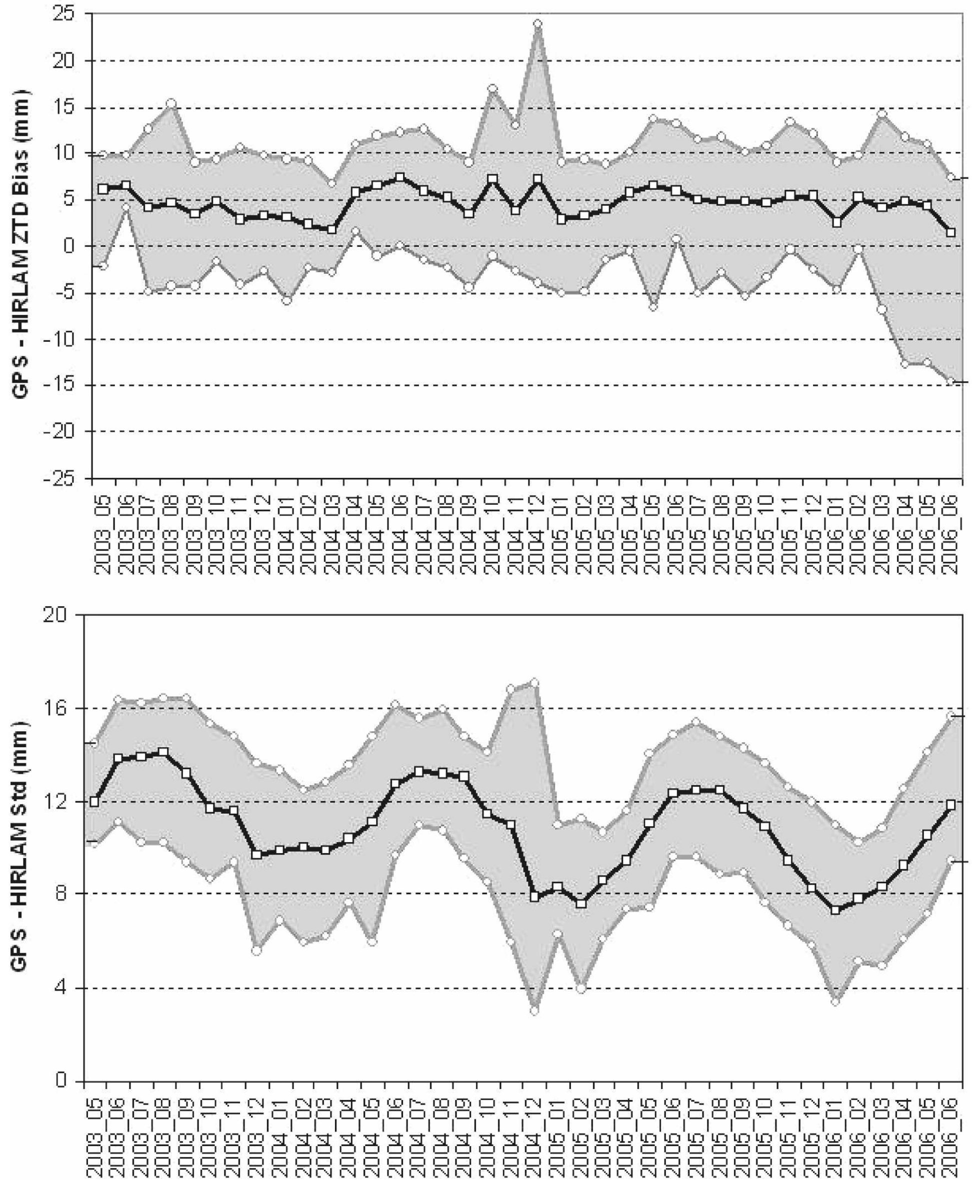

FIG. 11. (top) Monthly bias and (bottom) std dev of GPS ZTD vs HIRLAM ZTD for all the stations (black line). The gray area lies between the minimum and maximum values.

tainties of the different GPS ZTD estimates by comparing them with EUREF solutions. We realize that the uncertainties of the solutions coming out from the involved ACs are underestimated and, therefore, should be rescaled by a factors ranging from 1.4 to 5.8. Only the GAMIT solution (ACRI) has a rescaling factor less than one (~0.9). Another finding is that the closer the rescaling factor is to 1, the closer the residuals are to a normal distribution.

ZTD estimates from 13 GPS sites, where radiosonde profiles are available nearby, are compared for the period April 2003–June 2006. The overall bias is about 7 mm with GPS ZTD systematically higher than radiosonde ZTD. The standard deviation has a seasonal dependence, being higher in summer than in winter when more humidity is present. A night/day bimodal distribution in the GPS minus radiosonde ZTD bias is detected. The midday bias is higher than the midnight bias. Such evidence was also noted and discussed by Haase et al. (2003), where it was suggested that the bias is likely to be due to the day–night humidity bias present in the radiosonde measurement rather than in a humidity bias related to GPS measurements.

In the comparison statistics between the ZTD values extracted from the HIRLAM model, which assimilates the ZTD, and those derived from GPS NRT processing we have an average bias of about −4.8 mm and a standard deviation of 11.5 mm. The residuals between HIRLAM and GPS ZTD have a seasonal signal with a standard deviation higher in summer than in winter. The monthly ZTD standard deviation increases from about 5 mm in winter to about 15 mm in summer. The results of the statistical comparison between our ZTD estimates and HIRLAM have been confirmed by the results of the other TOUGH analysis centers. Other partners in the TOUGH consortium will be looking further at the impact of GPS ZTD on forecast improvement. We are able to state, however, that the current comparison using HIRLAM with assimilated GPS ZTD has a much smaller standard deviation than previous comparisons with HIRLAM without assimilated GPS ZTD, indicating that the driving the model in the direction of the GPS data is consistent with the other datasets that are being assimilated.

Acknowledgments. We acknowledge all the TOUGH analysis centers for providing the data used in this work. We thank Junhong (June) Wang (National Center for Atmospheric Research), Henrik Vedel (Danish Meteorological Institute), Jennifer Haase (Purdue University), and another anonymous reviewer for their helpful comments on this manuscript.

REFERENCES

Askne, J., and H. Nordius, 1987: Estimation of tropospheric delay for microwaves from surface weather data. *Radio Sci.,* **22,** 379–386.

Beutler, G., M. Rothacher, S. Schaer, T. A. Springer, J. Kouba, and R. E. Neilan, 1999: The international GPS service (IGS): An interdisciplinary service in support of earth sciences. *Adv. Space Res.,* **23,** 631–653.

——, and Coauthors, 2007: Bernese GPS software version 5.0. User Manual. Astronomical Institute, University of Bern, 636 pp.

Bevis, M., S. Businger, T. A. Herring, C. Rocken, R. A. Anthes, and R. H. Ware, 1992: GPS meteorology: Remote sensing of atmospheric water vapour using the global positioning system. *J. Geophys. Res.,* **97,** 15 787–15 801.

——, ——, S. Chiswell, T. A. Herring, R. A. Anthes, C. Rocken, and R. H. Ware, 1994: GPS meteorology: Mapping zenith wet delays onto precipitable water. *J. Appl. Meteor.,* **33,** 379–386.

Elgered, G., J. L. Davis, T. A. Herring, and I. I. Shapiro, 1991: Geodesy by radio interferometry: Water vapor radiometry for estimation of the wet delay. *J. Geophys. Res.,* **96,** 6541–6555.

——, H.-P. Plag, H. van der Marel, S. Barlag, and J. Nash, Eds., 2005: *COST 716 Final Report: Exploitation of Ground-Based GPS for Operational Numerical Weather Prediction and Climate Applications*. Institute of Applied Physics, University of Bern, 234 pp.

Emardson, T. R., and H. J. P. Derks, 1999: On the relation between the wet delay and the integrated precipitable water vapor in the European atmosphere. *Meteor. Appl.,* **6,** 1–12.

Guerova, G., E. Brockmann, F. Schubiger, J. Morland, and C. Mätzler, 2005: An integrated assessment of measured and modeled integrated water vapor in Switzerland for the period 2001–03. *J. Appl. Meteor.,* **44,** 1033–1044.

Haase, J., and Coauthors, 2001: The contributions of the MAGIC project to the COST 716 objectives of assessing the operational potential of ground-based GPS meteorology on an international scale. *Phys. Chem. Earth,* **26,** 433–437.

——, M. Ge, H. Vedel, and E. Calais, 2003: Accuracy and variability of GPS tropospheric delay measurements of water vapor in the western Mediterranean. *J. Appl. Meteor.,* **42,** 1547–1568.

Herring, T. A., R. W. King, and S. C. McClusky, 2006: GAMIT reference manual: GPS analysis at MIT. Release 10.3, MIT, 182 pp. [Available online at http://www-gpsg.mit.edu/~simon/gtgk/docs.htm.]

Kursinski, E. R., and G. A. Hajj, 2001: A comparison of water vapor derived from GPS occultations and global weather analyses. *J. Geophys. Res.,* **106,** 1113–1138.

Ohtani, R., and I. Naito, 2000: Comparisons of GPS-derived precipitable water vapors with radiosonde observations in Japan. *J. Geophys. Res.,* **105,** 26 917–26 929.

Pacione, R., 2005: ASI analysis centre. *COST 716 Final Report: Exploitation of Ground-Based GPS for Operational Numerical Weather Prediction and Climate Applications,* G. Elgered et al., Eds., Institute of Applied Physics, University of Bern, 35–37.

——, and F. Vespe, 2003: GPS zenith total delay estimation in the Mediterranean area for climatological and meteorological applications. *J. Atmos. Oceanic Technol.,* **20,** 1034–1042.

——, C. Sciarretta, F. Vespe, C. Faccani, R. Ferretti, E. Fionda, C. Ferraro, and A. Nardi, 2001: GPS meteorology: Validation and comparisons with ground-based microwave radiometer and mesoscale model for the Italian GPS permanent stations. *Phys. Chem. Earth,* **26,** 139–145.

Rood, H. J., 1982: Gravitational mechanics of systems of galaxies. I—Corrections for errors in redshifts. *Astrophys. J. Suppl. Ser.,* **49,** 111–147.

Saastamoinen, J., 1972: Atmospheric correction for the troposphere and stratosphere in radio ranging of satellites. *The Use of Artificial Satellites for Geodesy, Geophys. Monogr.,* Vol. 15, Amer. Geophys. Union, 247–251.

Sandage, A., 1978: Optical redshifts for 719 bright galaxies. *Astron. J.,* **83,** 904–937.

Santerre, R., 1991: Impact of GPS satellite sky distribution. *Manuscr. Geod.,* **16,** 28–53.

Springer, T. A., and U. Hugentobler, 2001: IGS ultra rapid products for (near-) real-time applications. *Phys. Chem. Earth,* **26,** 623–628.

Tonry, J., and M. Davis, 1979: A survey of galaxy redshifts. I—Data reduction technique. *Astron. J.,* **84,** 1511–1525.

Turner, D. D., B. M. Lesht, S. A. Clough, J. C. Liljegren, H. E. Revercomb, and D. C. Tobin, 2003: Dry bias and variability in Vaisala RS80-H radiosondes: The ARM experience. *J. Atmos. Oceanic Technol.,* **20,** 117–132.

Van Baelen, J., J.-P. Aubagnac, and A. Dabas, 2005: Comparison of near–real time estimates of integrated water vapor derived with GPS, radiosondes, and microwave radiometer. *J. Atmos. Oceanic Technol.,* **22,** 201–210.

Vömel, H., and Coauthors, 2006: Radiation dry bias of the Vaisala RS92 humidity sensor. *J. Atmos. Oceanic Technol.,* **24,** 953–963.

Wang, J., H. L. Cole, D. J. Carlson, E. R. Miller, K. Beierle, A. Paukkunen, and T. K. Laine, 2002: Corrections of humidity measurement errors from the Vaisala RS80 radiosonde—Application to TOGA COARE data. *J. Atmos. Oceanic Technol.,* **19,** 981–1002.

Webb, F. H., and J. F. Zumberge, 1997: An introduction to GIPSY/OASIS-II. JPL Publication D-11088.

WMO, 1996: *Guide to Meteorological Instruments and Methods of Observation.* 6th ed. World Meteorological Organization, 433 pp.

Zumberge, J. F., M. B. Heflin, D. C. Jefferson, M. M. Watkins, and F. H. Webb, 1997: Precise point positioning for the efficient and robust analysis of GPS data from large networks. *J. Geophys. Res.,* **102,** 5005–5017.